Intense γ-Ray Source in the Giant-Dipole-Resonance Range Driven by 10-TW Laser Pulses

A. Giulietti,[1,2] N. Bourgeois,[3] T. Ceccotti,[4] X. Davoine,[5] S. Dobosz,[4] P. D'Oliveira,[4] M. Galimberti,[1,*] J. Galy,[6]
A. Gamucci,[1,2] D. Giulietti,[1,2,7] L. A. Gizzi,[1,2] D. J. Hamilton,[6,+] E. Lefebvre,[5] L. Labate,[1,2] J. R. Marquès,[3] P. Monot,[4]
H. Popescu,[4] F. Réau,[4] G. Sarri,[1] P. Tomassini,[1,8] and P. Martin[4]

[1]*Intense Laser Irradiation Laboratory, IPCF, Consiglio Nazionale delle Ricerche, CNR Campus, Pisa, Italy*
[2]*INFN, Sezione di Pisa, Italy*
[3]*Laboratoire pour l'Utilisation des Lasers Intenses, CNRS UMR 7605, Ecole Polytechnique, Palaiseau, France*
[4]*CEA-DSM/DRECAM/SPAM, Gif sur Yvette Cedex, France*
[5]*Département de Physique Théorique et Appliquée, CEA/DIF, 91680 Bruyères-le-Châtel, France*
[6]*European Commission, JRC Institute for Transuranium Elements, Karlsruhe, Germany*
[7]*Dipartimento di Fisica, Università di Pisa, Pisa, Italy*
[8]*INFN, Sezione di Milano, Italy*
(Received 16 November 2007; published 3 September 2008)

A γ-ray source with an intense component around the giant dipole resonance for photonuclear absorption has been obtained via bremsstrahlung of electron bunches driven by a 10-TW tabletop laser. 3D particle-in-cell simulation proves the achievement of a nonlinear regime leading to efficient acceleration of several sequential electron bunches per each laser pulse. The rate of the γ-ray yield in the giant dipole resonance region ($8 < E_\gamma < 17.5$ MeV) was measured, through the radio activation of a gold sample, to be 4×10^8 photons per joule of laser energy. This novel all-optical, compact, and efficient electron-γ source is suitable for photonuclear studies and medical uses.

Photonuclear reactions involving γ rays of energy in the range 15–30 MeV [the giant dipole resonance (GDR) of medium and heavy nuclei for photoabsorption [1–3]] are of primary relevance for nuclear studies. The GDR enables the production of radionuclides at rates of practical interest via photonuclear reactions with reasonable γ-ray intensities. In a wider energy range (from a few to several tens of MeV), both γ rays and electrons are used in a variety of applications, from sterilization to cancer therapy. In all of these cases, γ rays are generated via bremsstrahlung in a suitable dumper (the "radiator"), by relativistic electron bunches accelerated by dedicated accelerators. To this purpose, specialized linear electron accelerators are operating in many hospitals [4]. A further option under examination is to use such accelerators and the bremsstrahlung yield to produce (γ, n) reactions for neutron therapy [5]. This explains why special attention has been devoted recently to laser-driven electron accelerators for the production of γ rays [6].

The general objective of building-up laser-driven plasma accelerators was promoted by the theoretical Letter from Tajima and Dawson [7]. After the first encouraging results [8,9], an exponential rate of successes led to the production of quasimonochromatic multi-MeV [10] up to GeV electron bunches [11]. However, relevant tasks have still to be pursued, including achievement of stability and reproducibility of the laser driving process [12].

We limited our objective to find a regime suitable for the setup of a small all-optical laser-driven accelerator able to efficiently generate via bremsstrahlung γ rays in a given spectral range. Within this limit, most of the requirements on the electron bunches are considerably relaxed. Monochromaticity, small divergence, pointing stability, etc. are requested at a moderate level, while the main effort has to be devoted to the efficiency and reliability of the process. A number of experiments have been performed in the past decade with the common objective of obtaining laser-driven nuclear reactions [13]. Most of those experiments have used very high power pulses, from 40 to 100 TW [14–17] up to PW [18,19], delivered by laser systems not suitable for practical applications. In some cases smaller lasers have been used in tight focusing regime [20,21]. In these latter cases, the electron yield was limited to tens of pC per joule of laser energy with poor reproducibility.

We found for the first time, with a 10 TW laser, a regime of electron acceleration of high efficiency (nC/J). Although the electron spectrum was not exactly reproducible from shot to shot, the spectrum averaged over a large number of shots makes our tabletop accelerator suitable for practical applications and for driving our intense γ-ray source.

Our accelerator delivers high-charge (nC/J), reproducible, fairly collimated, and quasimonochromatic electron bunches, whose peak energy moves shot by shot in the range 10–45 MeV; such an energy range is very suitable for driving a γ-ray source in the GDR spectral region. We first describe these electron bunches and show that their energy range as well as the efficiency of the process are well explained by a 3D simulation. Finally, we characterize the electron-driven γ-ray source in terms of yield and

spectrum as they were deduced by postprocessing measurements after the activation of a gold sample.

The laser-driven electron accelerator was set up at the SLIC facility (CEA-Saclay, France) with the UHI-10 Ti: sapphire laser, which delivered 65 fs chirped pulse amplification pulses with energy up to 0.7 J at a wavelength of $\lambda_0 = 800$ nm. The pulses were focused by an $f/5$ off-axis parabolic mirror producing a quasi-Gaussian spot where the normalized field parameter was nominally $a_0 \lesssim 2$. The nanosecond-scale contrast ratio of the pulse ($>10^6$) ensured that no preplasma was formed by amplified spontaneous emission.

Supersonic gas-jet nozzles of diameters ranging from 0.6 to 6.0 mm were tested in a wide range of helium backing pressures. The results reported in the present Letter were obtained in what was found to be the optimum conditions, namely, a 4 mm nozzle with 25 bar backing pressure, corresponding to an atomic density of 10^{19} cm^{-3} at 0.5 mm from the nozzle exit, i.e., the position of the laser axis. The laser pulse was linearly polarized along the gas flow axis.

Diagnostics of the plasma included interferometry with a probe perpendicular to the propagation axis. The Mach-Zehnder interferometer was operated with a small portion of the femtosecond pulse, doubled in frequency, in the same way as in a previous experiment on propagation and ionization studies [22,23]. The electron density along the pulse path was measured to be $n_e \approx 2 \times 10^{19}$ cm^{-3}. At this density the electron plasma wave has a period $T_p \approx 25$ fs and wavelength $\lambda_p \approx 7.5$ μm. A Lanex screen, placed at a distance of 44 mm from the focal plane and shielded from light by a 0.3 mm copper foil, provided the overall spatial distribution of the electrons. A magnetic spectrometer coupled with Lanex provided the shot-to-shot electron energy spectrum. A spatial high-energy electron beam analyzer (SHEEBA) device [24] provided the angular distribution of each spectral component. Finally, a photonuclear activation setup via induced bremsstrahlung provided a precise measurement of the electron bunch charge via Monte Carlo code deconvolution. This latter setup also provided the measurement on the γ-ray source yield. The Lanex screen was essential for "tuning" the electron accelerator; once tuned, the electron bunch parameters including divergence, spectrum, and charge were measured with SHEEBA, magnetic spectrometer, and nuclear activation.
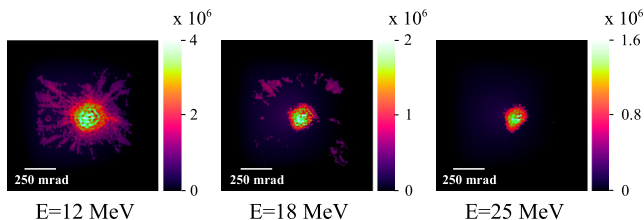
SHEEBA raw data were analyzed with an original algorithm [24] based on the particle transport Monte Carlo code GEANT-4 [25]. The algorithm transforms the raw patterns produced by the electrons in the radiochromic films into the spatial distribution of electrons for each energy component. Figure 1 shows three data obtained in this way: they correspond to electron energies of interest for bremsstrahlung in the GDR range, namely, 12, 18, and 25 MeV, integrated over ten consecutive shots. Analysis of data from all films leads to an energy spectrum showing for this particular series of shots, a high-energy peak at 12 MeV, 8 MeV in width.

Figure 2 shows a typical electron spectrum for a single laser shot measured with the magnetic spectrometer. Figure 2(a) is the raw spectrum recorded in the Lanex screen, with electron deflection along the horizontal axis. Figure 2(b) shows the normalized lineout of the Lanex signal. In this particular spectrum, a peaked high-energy component at 16 MeV with a FWHM of 8 MeV can be seen. Such a quasimonoenergetic structure was always observed in a series of hundreds of laser shots over several days. However, the position of the peak varied unpredictably in a range from 10 to 45 MeV while the peak width was systematically less than 10 MeV. As for the electron bunch collimation, Lanex, SHEEBA, and magnetic spectrometer provided self-consistent data. Electrons produced by a single laser shot were collimated within an angle of 30 mrad FWHM, while the pointing direction of the electron beam over several tens of shots was within an angle of less than 100 mrad FWHM.

FIG. 1 (color online). Spatially resolved spectral data of the accelerated electrons from the SHEEBA detector.
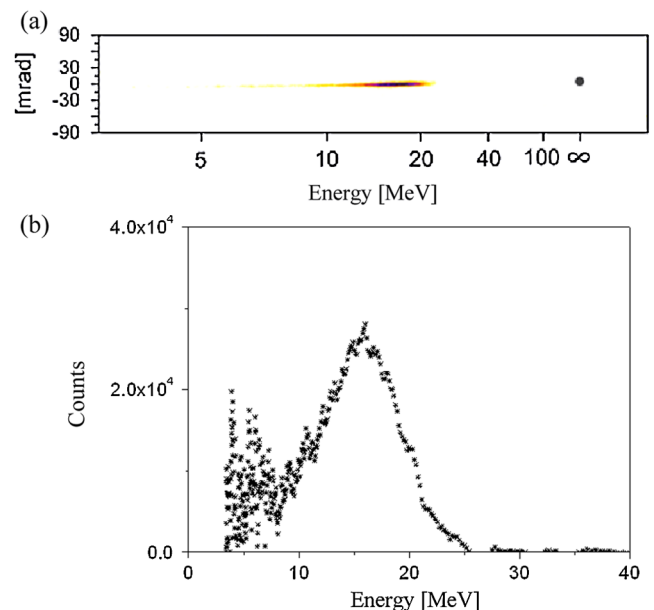

FIG. 2 (color online). Typical electron spectrum obtained by the magnetic spectrometer.

The electron bunches were converted into high-energy bremsstrahlung photons in a 2 mm thick tantalum radiator. In order to measure both the electron bunch charge and the γ-ray production rate, the bremsstrahlung photons were used for activation of a 4 mm thick gold sample. We point out here that the cross section for the ^{197}Au$(\gamma, n)^{196}$Au reaction peaks (GDR) at about 13 MeV [26] with a maximum of around 570 mb and a characteristic width of around 5 MeV FWHM, matching very well the bremsstrahlung spectrum of our electrons in the 10–45 MeV range. The two planar samples were aligned parallel to each other and on axis with the electron beam, at 35 and 50 mm from the laser focus, respectively. In total, 106 laser shots were taken on target during this phase of the experiment, inducing (γ, n) reactions on the ^{197}Au sample and leading to a total ^{196}Au yield of 49.6 ± 2.1 Bq. This activity was determined using postirradiation gamma spectroscopy of the activated sample with a high-purity germanium detector (based on the 333 and 355 keV γ lines associated with the ^{196}Au decay).

The measured photonuclear activity was convoluted with the electron spectrum and divergence results given above to calculate the photon flux incident on the gold sample (using a Monte Carlo procedure described in [6]). The shot-to-shot variation of the electron energy was taken into account in the Monte Carlo calculation by using an electron spectrum integrated over 22 consecutive shots. This integrated spectrum was found to peak at 21 MeV, with a FWHM energy spread of 18 MeV showing again that our accelerator is suitable for driving a γ-ray source in the GDR region. The spectrum of the radiation produced by bremsstrahlung was also calculated: it is shown in Fig. 3. The calculated γ-ray yield in the energy range 8–17.5 MeV was $(3.74 \pm 0.14) \times 10^8$ photons per joule of laser energy. From the photon flux also the absolute number of bunch electrons could be determined. The total number of electrons (with $E > 8$ MeV, the ^{197}Au$(\gamma, n)^{196}$Au
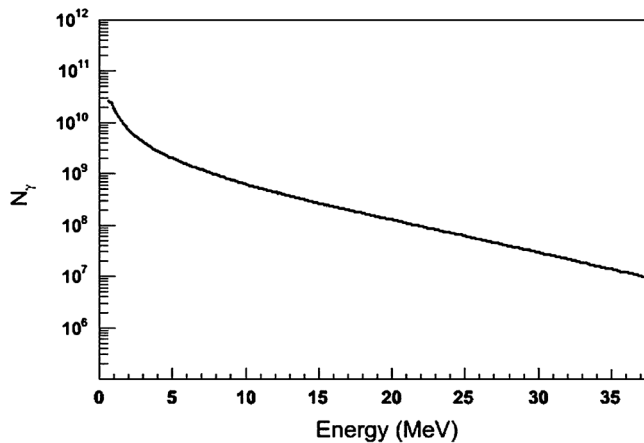

FIG. 3. Spectrum of the γ radiation produced by the electron bunches crossing the 2 mm tantalum slab, as calculated from the postprocessing activity measurements.

reaction threshold) calculated in this way was found to be $7.32 \pm 0.26 \times 10^9$ per laser shot (corresponding to $\approx 10^{10}$ electrons per joule of laser energy). A further contribution from systematic errors associated with detector acceptance corrections, shot-to-shot variation, and calculation uncertainties has been estimated to be below 15%. The total number of electrons involved in the nuclear process is consistent with SHEEBA data, that give about 10^{11} electrons of energy above 7.5 MeV collected in 10 shots, with a total relative error of the order of 40%.

A numerical simulation of our electron accelerator has been performed with the 3D particle-in-cell code CALDER [16]. It has been indeed pointed out by previous works that only full 3D simulations can account for the three-dimensional effects that interplay in the nonlinear wakefield problem [27]. Some snapshots of the simulation are reproduced in Fig. 4. The simulated laser field distribution (not reported here) shows a first stage of modest self-focusing and temporal compression of the pulse, with nonlinear excitation of plasma waves. Then, self-phase modulation and pulse compression split the original pulse into pulselets. These two phenomena lead to an increase of the plasma wave amplitude. Approximately 2.5 mm after the entrance in the plasma, the laser pulse undergoes significant depletion and defocusing. The simulated electron density shows a nonlinear plasma wave growth with a clear progressive transverse bending of the wave front. The plasma wave reaches the wave breaking limit (5×10^{11} V/m) and electrons originating from the back of the first plasma wave period are injected into the accelerating region of the wave. The latter stage is shown by Fig. 4(a) (electron density distribution when the pulse is about 1.65 mm after the entrance) where the electron bunches with $E > 5$ MeV are identified by the blue contour lines. We stress here that most of the electrons are efficiently accelerated in the third and fourth plasma periods. Electron injection in buckets behind the first plasma period was originally found in a simulation work in condition of transverse wave breaking [28].

The snapshots in Figs. 4(b)–4(d) show the electron momentum distribution along the propagation axis when the pulse is at about 1 mm [4(b)], 2 mm [4(c)], and 2.5 mm [4(d)], respectively. The electron bunches are accelerated up to 42 MeV, then the laser pulse depletion stops the plasma wave growth. Thus, the electron bunches are no longer accelerated and propagate in the last part of the gas jet, remaining quasimonoenergetic and collimated. The nonlinear character of the process accounts for the shot-to-shot fluctuation in the peak energy observed in the experiment, while the multiple-bunch acceleration in several plasma wave periods accounts for the high efficiency.

In conclusion, we have set up and tested a novel, efficient, all-optical accelerator of relativistic electron bunches whose spectrum, integrated over many shots, allowed us to create a γ-ray source with a relevant compo-

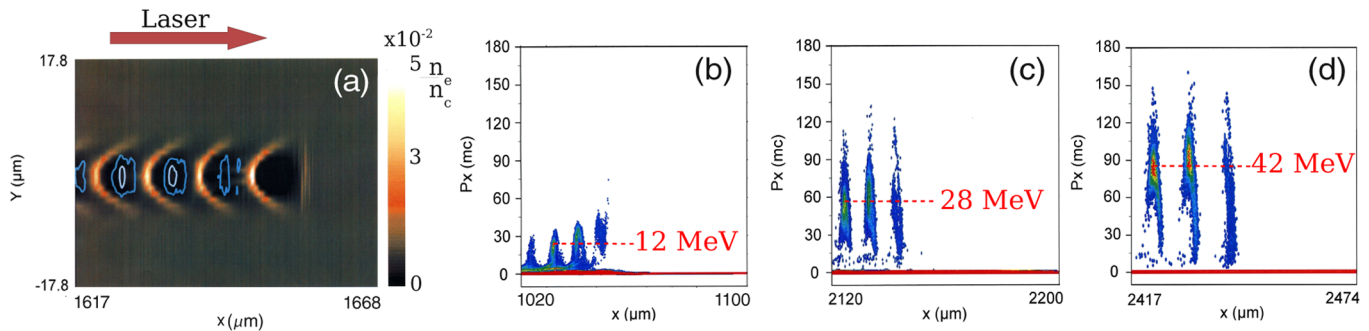P H Y S I C A L   R E V I E W   L E T T E R S

FIG. 4 (color online).   Snapshots from the 3D simulation. (a) Electron density distribution when the laser pulse is at about 1.65 mm after the entrance in the gas jet. (b)–(d) Electron momentum distribution along the propagation axis when the laser pulse is at 1, 2, and 2.5 mm, respectively.

nent located about the GDR. The interest of such an electron and gamma source lies in the reliability of the techniques involving a tabletop laser and a gas jet. This twofold (electrons or γ rays) source can compete with the existing small scale conventional accelerators in a variety of operational contexts like scientific laboratories, industry, and hospitals. As an example, accelerators used for the intraoperatory radiotherapy (IORT) of cancer [29] deliver typically mean electronic currents comparable to those delivered by our laser-driven accelerator. The LIAC system for IORT by Sordina S.r.l. [30] delivers 18 nA at 10 Hz of electrons of 12 MeV, within an acceleration length of 900 mm. Our accelerator delivers 16 nA at 10 Hz of ~ 20 MeV electrons within an acceleration length ≤ 4 mm. Many accelerators devoted to γ sources used for sterilization and for industrial radiography have similar performances. Finally, an obvious advantage for an all-optical laser-driven accelerator is that only a small part of the equipment needs radioprotection for the operator.

*Present address: Central Laser Facility, Rutherford Appleton Laboratory, Didcot, Oxon, UK.

+Present address: Department of Physics and Astronomy, University of Glasgow, Glasgow, UK.
[1] W. Bothe and W. Gentner, Z. Phys. **106**, 236 (1937).
[2] G. C. Baldwin and G. S. Klaiber, Phys. Rev. **71**, 3 (1947); G. C. Baldwin and G. S. Klaiber, Phys. Rev. **73**, 1156 (1948).
[3] J. Speth and A. Van Der Woude, Rep. Prog. Phys. **44**, 719 (1981).
[4] D. I. Thwaites and J. B. Tuohy, Phys. Med. Biol. **51**, R343 (2006).
[5] G. L. Locher, Am. J. Roentgenol. **36**, 1 (1936); C. Ongaro et al., Phys. Med. Biol. **45**, L55 (2000).
[6] J. Galy et al., New J. Phys. **9**, 23 (2007).
[7] T. Tajima and J. M. Dawson, Phys. Rev. Lett. **43**, 267 (1979).
[8] A. Modena et al., Nature (London) **377**, 606 (1995).
[9] D. Giulietti et al., Phys. Plasmas **9**, 3655 (2002).
[10] S. P. D. Mangles et al., Nature (London) **431**, 535 (2004); C. G. R. Geddes et al., Nature (London) **431**, 538 (2004); J. Faure et al., Nature (London) **431**, 541 (2004).
[11] W. P. Leemans et al., Nature Phys. **2**, 696 (2006).
[12] A. Giulietti et al., Laser Part. Beams **25**, 513 (2007).
[13] F. Ewald, Lect. Notes Phys. **694**, 25 (2006).
[14] S. A. Reed et al., Appl. Phys. Lett. **89**, 231107 (2006).
[15] S. A. Reed et al., J. Appl. Phys. **102**, 073103 (2007).
[16] E. Lefebvre et al., Nucl. Fusion **43**, 629 (2003).
[17] Y. Glinec et al., Phys. Rev. Lett. **94**, 025003 (2005).
[18] T. E. Cowan et al., Phys. Rev. Lett. **84**, 903 (2000).
[19] K. W. D. Ledingham et al., Science **300**, 1107 (2003).
[20] B. Liesfeld et al., Appl. Phys. B **79**, 1047 (2004).
[21] B. Hidding et al., Phys. Rev. Lett. **96**, 105004 (2006).
[22] A. Giulietti et al., Phys. Plasmas **13**, 093103 (2006).
[23] L. A. Gizzi et al., Phys. Rev. E **74**, 036403 (2006).
[24] M. Galimberti et al., Rev. Sci. Instrum. **76**, 053303 (2005).
[25] S. Agostinelli et al., Nucl. Instrum. Methods Phys. Res., Sect. A **506**, 250 (2003).
[26] IAEA Photonuclear Data Library, http://www-nds.iaea.org/photonuclear.
[27] F. S. Tsung et al., Phys. Plasmas **13**, 056708 (2006).
[28] S. V. Bulanov et al., Phys. Rev. Lett. **78**, 4205 (1997).
[29] U. Veronesi et al., Breast J. **9**, 106 (2003).
[30] http://www.sordina.com